Quantum tunneling recombination in a system of randomly distributed trapped electrons and positive ions

2017 J. Phys.: Condens. Matter 29 365701

(http://iopscience.iop.org/0953-8984/29/36/365701)

IOP Publishing Journal of Physics: Condensed Matter
J. Phys.: Condens. Matter **29** (2017) 365701 (8pp) https://doi.org/10.1088/1361-648X/aa7db5

Quantum tunneling recombination in a system of randomly distributed trapped electrons and positive ions

Vasilis Pagonis[1], Christopher Kulp[2], Charity-Grace Chaney[1] and M Tachiya[3]

[1] Physics Department, McDaniel College, Westminster, MD 21157, United States of America
[2] Department of Astronomy and Physics, Lycoming College, Williamsport, PA 17701, United States of America
[3] National Institute of Advanced Industrial Science and Technology (AIST), AIST Tsukuba Central 5, Tsukuba, Ibaraki 305-8565, Japan

E-mail: vpagonis@mcdaniel.edu (V Pagonis) and m.tachiya@aist.go.jp (M Tachiya)

Received 5 May 2017, revised 30 June 2017
Accepted for publication 5 July 2017
Published 7 August 2017

Abstract

During the past 10 years, quantum tunneling has been established as one of the dominant mechanisms for recombination in random distributions of electrons and positive ions, and in many dosimetric materials. Specifically quantum tunneling has been shown to be closely associated with two important effects in luminescence materials, namely long term afterglow luminescence and anomalous fading. Two of the common assumptions of quantum tunneling models based on random distributions of electrons and positive ions are: (a) An electron tunnels from a donor to the nearest acceptor, and (b) the concentration of electrons is much lower than that of positive ions at all times during the tunneling process. This paper presents theoretical studies for arbitrary relative concentrations of electrons and positive ions in the solid. Two new differential equations are derived which describe the loss of charge in the solid by tunneling, and they are solved analytically. The analytical solution compares well with the results of Monte Carlo simulations carried out in a random distribution of electrons and positive ions. Possible experimental implications of the model are discussed for tunneling phenomena in long term afterglow signals, and also for anomalous fading studies in feldspars and apatite samples.

Keywords: quantum tunneling recombination, luminescence afterglow model, luminescence anomalous fading

(Some figures may appear in colour only in the online journal)

1. Introduction

Extensive experimental and modeling work during the past decade has shown that quantum mechanical tunneling is closely associated with the 'long term afterglow' signals (AG) in luminescence materials, and also with the related phenomenon of 'anomalous fading' (AF) of luminescence signals in feldspars and apatites [1–26]. Different types of mechanisms have been investigated, namely, direct tunneling from the ground state of the trapped electron, as well as tunneling taking place via the excited state of the system of electron–hole pairs. In addition, two possible complementary modeling approaches have been used in the literature to study theoretically tunneling in random distribution of defects: an approach using a differential equation, and a second approach based on Monte Carlo simulations.

The basic framework of modeling in this research area has been the description of tunneling phenomena in these materials, based on a random distribution of electrons and positive charges [1, 2]. The basic physical assumptions in the

models are (a) An electron tunnels from a donor to the nearest acceptor (nearest-neighbor tunneling), and (b) The concentration of positive ions far exceeds that of electrons in the system. The differential equation description of tunneling in these random distributions is now well established, and analytical equations have been derived which describe the loss of charge during the luminescence process. For a recent review of modeling work in this area, the reader is referred to the recent review by Pagonis *et al* [10].

A second modeling approach of luminescence in random distributions of charges is based on Monte Carlo techniques. Larsen *et al* [7] presented a numerical Monte Carlo model that simulates the processes of charge loss, charge creation and charge recombination in feldspar. These authors also used the assumption of nearest-neighbor tunneling. Their model assumed that the concentration of electrons and positive ions are equal at all times. Pagonis and Kulp [17] presented a different version of the Monte Carlo model in which the concentration of positive ions far exceeds that of electrons, and the results from their model compared well with the analytical equation originally derived by Tachiya and Mozumder [1].

This paper presents an effort to describe tunneling processes in random distributions in a more general case, by studying the effect of varying the relative concentrations of electrons and positive ions in the solid. The specific goals of this paper are:

- To derive appropriate differential equations which can describe quantitatively the loss of charge due to tunneling, for arbitrary relative concentrations of electrons and positive ions in the solid.
- To solve these differential equations analytically.
- To compare the analytical solutions of the differential equations with Monte Carlo simulations of quantum tunneling.
- To discuss possible experimental implications for the quantitative description of AF and AG signals in dosimetric materials, including feldspars and apatites.

2. Electron tunneling from trapped electrons to positive ions in a solid in which they are initially distributed randomly

A model for ground-state tunneling in a completely random distribution of electrons and positive ions was first developed by Tachiya and Mozumder [1, 2]. Their model is based on the physical assumption that the concentration of positive ions in the solid is much higher than that of trapped electrons. Because of this assumption, the concentration of *positive ions* would remain practically constant during the tunneling process, and it can be used to characterize the system.

In this section we examine the decay kinetics of trapped electrons by tunneling to positive ions, for arbitrary relative concentrations of trapped electrons and positive ions. We assume that trapped electrons are randomly distributed relative to other trapped electrons in the system, and that positive ions are randomly distributed relative to other positive ions. We further assume that trapped electrons and positive ions are mutually randomly distributed.

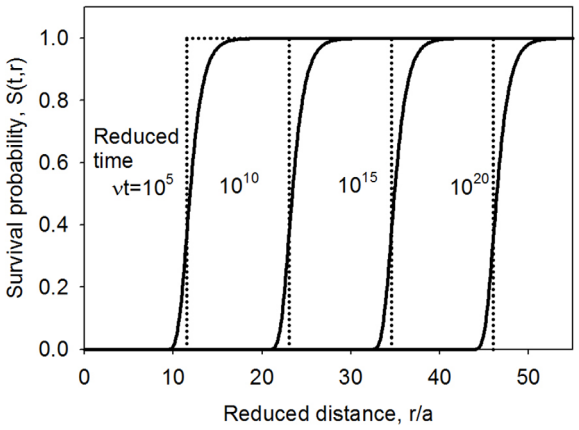

Figure 1. The survival probability $S(t, r)$ given by equation (2) is plotted as a function of the reduced distance (r/a) and for widely differing values of the reduced time νt. Equation (4) is shown by the dotted lines.

We denote the concentrations of trapped electrons at time zero and t as n_0 and $n(t)$, respectively (in units of trapped electrons or positive ions per m^3). The concentration $n(t)$ decreases with time, and the goal of this section is to derive a differential equation for $n(t)$. Under the above assumptions, we can calculate the decay of trapped electrons in the following way.

The tunneling process is described by two parameters, the frequency factor ν (s^{-1}) characterizing the tunneling process and the tunneling length a (m). The rate constant $k(r)$ for electron tunneling between a trapped electron and a positive ion separated by r is given by:

$$k(r) = \nu \exp(-r/a). \tag{1}$$

The survival probability $S(t,r)$ at time t of a trapped electron and a positive ion separated by a distance r is given by:

$$S(t, r) = \exp[-k(r)t] = \exp[-\nu t \exp(-r/a)]. \tag{2}$$

Figure 1 shows the survival probability $S(t, r)$ of a trapped electron and a positive ion separated by a reduced distance r/a, as a function of reduced time νt. The function $S(t, r)$ shown in figure 1 indicates that at any given time t there is a critical distance $r(t)$ up to which $S(t, r)$ is approximately zero, and beyond which this probability is essentially unity. We try to reproduce this behavior by using a simple function. We approximate $S(t,r)$ as

$$S(t, r) = 1 \quad \text{for } \nu t \exp(-r/a) < 1 \tag{3a}$$

$$S(t, r) = 0 \quad \text{for } \nu t \exp(-r/a) > 1. \tag{3b}$$

Although the approximation that $e^{-x} = 1$ for $x < 1$ and $e^{-x} = 0$ for $x > 1$ is in general a crude approximation, equations (3*a*) and (3*b*) give a rather good approximation because the term $\nu t \exp(-r/a)$ changes rapidly with r. If we re-express the criterion in equation (3) by using r, equation (3) is rewritten as

$$S(t, r) = 1 \quad r > r(t) \tag{4a}$$

$$S(t, r) = 0 \quad r < r(t) \tag{4b}$$

where the critical distance $r(t)$ is a function of time and given by

$$r(t) = a\ln(\nu t). \tag{4c}$$

Equation (4) is shown by the dotted lines in figure 1. The exact $S(t, r)$ curves shown by the full lines in figure 1 are well approximated by the dotted lines. It is known that the approximation given by equation (4) gives reasonable results in the calculations of other types of reactions, which also occur by electron tunneling [1, 2]. Figure 1 and equation (4) indicate that at any given time t electron tunneling from a trapped electron to a positive ion occurs practically exclusively to a positive ion separated from the trapped electron by a distance $r(t)$ given by equation (4c).

2.1. Case of equal initial concentrations of trapped electrons and positive ions

If the initial concentrations of trapped electrons and positive ions are equal, their concentrations at time t are also equal. We denote the concentrations of trapped electrons and positive ions at time t both as $n(t)$. Then the number of positive ions at a distance $r \sim r + \mathrm{d}r$ from a trapped electron is given by $4\pi n(t)r^2\mathrm{d}r$. The total electron tunneling rate from the trapped electron to any one of the positive ions at a distance $r \sim r + \mathrm{d}r$ from the trapped electron is given by $[4\pi n(t)r^2\mathrm{d}r]k(r)$. The decrease $\mathrm{d}n(t)$ of trapped electrons during time $t \sim t + \mathrm{d}t$ is given by the product of the concentration $n(t)$ of trapped electrons at time t, and the total electron tunneling rate $[4\pi n(t)r^2\mathrm{d}r]k(r)$ from each trapped electron:

$$\mathrm{d}n(t) = -\left[4\pi n(t)r^2\mathrm{d}r\right]k(r)n(t). \tag{5a}$$

Note that distance r in equation (5a) is related to time t through equation (4c). Equation (4c) gives a negative value for r, if t is smaller than ν^{-1}. To avoid this defect we make an approximation that if t is smaller than ν^{-1}, no tunneling occurs at all, and modify equation (5a) as

$$\mathrm{d}n(t) = -\left[4\pi n(t)r^2\mathrm{d}r\right]k(r)n(t) \tag{5b}$$

$$n(t) = n_0 \quad \text{for } t < \nu^{-1}. \tag{5c}$$

If one introduces equations (4c) in (5b), one obtains

$$\mathrm{d}n(t) = -4\pi a^3 n(t)^2 \mathrm{e}^{-\ln(t)}[\ln(\nu t)]^2\mathrm{d}t \tag{6a}$$

$$n(t) = n_0 \quad \text{for } t < \nu^{-1}. \tag{6b}$$

Equation (6) is a differential equation for tunneling phenomena, which is applicable when the concentrations of electrons and positive ions are equal at all times. The analytical solution of equation (6) is given by:

$$n(t) = 1/\left[\frac{1}{n_0} + 4\pi a^3 \int_{\nu^{-1}}^{t} \mathrm{e}^{-\ln(\nu t)}[\ln(\nu t)]^2\nu\mathrm{d}t\right] \tag{7a}$$

which reduces to

$$n(t) = 1/\left[\frac{1}{n_0} + (4\pi/3)a^3[\ln(\nu t)]^3\right] \tag{7b}$$

where we have used $n(\nu^{-1}) = n_0$. Equation (7b) can be rewritten as follows in terms of the survival probability given by $P(t) = n(t)/n_0$, where $n(t)$ and n_0 are the concentrations of trapped electrons at time t and zero, respectively.

$$P(t) = 1/\left\{1 + (4\pi/3)\,n_0 a^3[\ln(\nu t)]^3\right\} \tag{8a}$$

which is alternatively expressed as:

$$\frac{1}{P(t)} - 1 = (4\pi/3)n_0 a^3[\ln(\nu t)]^3. \tag{8b}$$

It is interesting to compare the kinetics described by equation (8b) with that of a second-order reaction. Consider a second order reaction $A + B \rightarrow C$. If the initial concentrations of A and B are equal, their concentrations at time t are also equal. If we denote it as $n(t)$, the kinetics of a second-order reaction is described by

$$\mathrm{d}n(t)/\mathrm{d}t = -kn(t)^2 \tag{9}$$

where k is the rate constant. The solution of this equation is given by

$$\frac{1}{P(t)} - 1 = n_0 kt. \tag{10}$$

Here n_0 is the initial concentrations of A and B, and $P(t) = n(t)/n_0$ stands for the survival probability throughout this paper. One can see that equation (8b) is similar to equation (10), except that the argument of the exponential function on the right-hand side of equation (10) has a linear t-dependence, while that of equation (8b) has a much slower logarithmic t-dependence (to the third power). Because of this logarithmic t-dependence the reaction described by equation (8b) effectively continues for much longer times than that described by equation (10).

2.2. Case of different initial concentrations of trapped electrons and positive ions

We denote the concentrations of trapped electrons at time zero and at time t as n_0 and $n(t)$, respectively. We also denote the concentrations of positive ions at time zero and at time t as m_0 and $m(t)$, respectively. The concentrations $m(t)$ and $n(t)$ are related through conservation of charge:

$$m(t) = m_0 - [n_0 - n(t)] = m_0 - n_0 + n(t). \tag{11}$$

The number of positive ions at a distance $r \sim r + \mathrm{d}r$ from a trapped electron at time t is given by $4\pi m(t)r^2\mathrm{d}r$. The total electron tunneling rate from the trapped electron to any one of the positive ions at a distance $r \sim r + \mathrm{d}r$ from the trapped electron is given by $[4\pi m(t)r^2\mathrm{d}r]k(r)$. The decrease $\mathrm{d}n(t)$ of trapped electrons during time $t \sim t + \mathrm{d}t$ is generally given by the product of the concentration $n(t)$ of trapped electrons at time t, and the total electron tunneling rate $[4\pi m(t)r^2\mathrm{d}r]k(r)$ from the trapped electron as:

$$\mathrm{d}n(t) = -\left[4\pi m(t)r^2\mathrm{d}r\right]k(r)n(t) \tag{12a}$$

$$n(t) = n_0 \quad \text{for } t < \nu^{-1}. \tag{12b}$$

We now consider two different situations, depending on the relative concentrations of electrons and positive ions.

2.2.1. Case in which the initial concentration of positive ions is much higher than that of trapped electrons. In this case the decrease of positive ions by recombination with trapped electrons is negligible, so we can approximate the concentration $m(t)$ of positive ions at time t by its initial value m_0. By using this approximation and equation (4*c*), we have from equation (12)

$$\mathrm{d}n(t) = -4\pi a^3 m_0 n(t) \mathrm{e}^{-\ln(\nu t)} [\ln(\nu t)]^2 \nu \mathrm{d}t \qquad (13a)$$

$$n(t) = n_0 \quad \text{for } t < \nu^{-1}. \qquad (13b)$$

The solution of this differential equation is given by :

$$P(t) = \exp\{-(4\pi/3) m_0 a^3 [\ln(\nu t)]^3\}. \qquad (14)$$

This equation was first derived by Tachiya and Mozumder [1], to describe the decay kinetics of trapped electrons by tunneling to randomly distributed scavengers whose concentration is much higher than that of trapped electrons. Note that in this case the survival probability $P(t)$ of trapped electrons depends on the initial concentration m_0 of positive ions, but does not depend on the initial concentration n_0 of electrons.

It is interesting once more to compare the kinetics described by this equation with that of a first-order reaction. Consider a first-order reaction $A \rightarrow C$. The kinetics of a first-order reaction is given by:

$$P(t) = \exp[-k't] \qquad (15)$$

where $P(t)$ is the survival probability and k' is the rate constant. We can see that equation (14) is similar to equation (15), except that the right-hand side of equation (15) has a linear t-dependence, while that of equation (14) has a much slower logarithmic t-dependence (to the third power). The logarithmic t-dependence is of course a consequence of tunneling.

2.2.2. Case in which the initial concentration of positive ions are higher, but not much higher than that of trapped electrons. We assume that the initial concentration m_0 of positive ions is higher than the initial concentration n_0 of trapped electrons. By introducing equation (11) in equation (12*a*) and using equation (4*c*), we obtain

$$\mathrm{d}n(t) = -4\pi a^3 [m_0 - n_0 + n(t)] \mathrm{e}^{-\ln(\nu t)} [\ln(\nu t)]^2 \nu \mathrm{d}t \qquad (16a)$$

$$n(t) = n_0 \quad \text{for } t < \nu^{-1}. \qquad (16b)$$

The solution of this differential equation is given by

$$P(t) = 1/\left\{-\frac{n_0}{m_0 - n_0} + \frac{m_0}{m_0 - n_0} \exp\left[\left(\frac{4\pi}{3}\right)(m_0 - n_0) a^3 [\ln(\nu t)]^3\right]\right\}. \qquad (17)$$

This equation reduces to equation (14) when m_0 is much higher than n_0, as expected.

3. Graphical presentation of the results obtained by using the analytical method

In this section we graphically present the results obtained by using the analytical method.

It is convenient to introduce the reduced initial concentration n_0' and the reduced time t' defined by:

$$n_0' = n_0 a^3 \quad t' = \nu t. \qquad (18)$$

If one uses these quantities, equation (8*a*) is simplified to:

$$P(t') = 1/\left\{1 + \left(\frac{4\pi}{3}\right) n_0' [\ln(t')]^3\right\} \qquad (19)$$

where $P(t) = n(t)/n_0$ is the survival probability of trapped electrons (or positive ions) and n_0' is the reduced initial concentration of trapped electrons (or positive ions) defined by equation (18).

Equation (19) depends only on the values of the reduced initial concentration $n_0' = n_0 a^3$ and the reduced time $t' = \nu t$, rather than on the individual values of the parameters (ν, a, n_0). Equation (19) is shown in figure 2(a) for three values of the reduced initial concentration of trapped electrons, $n_0' = 0.01$, 0.003 and 0.001. The three curves are normalized at time $t = 1/\nu$. As the value of n_0' increases, the loss of charge by tunneling becomes faster.

Figure 2(b) shows the normalized derivative $L(t) = -\mathrm{d}P/\mathrm{d}t$ for the same three values of the reduced initial concentrations of trapped electrons n_0', as those used in figure 2(a). The quantity $L(t) = -\mathrm{d}P/\mathrm{d}t$ is important from an experimental point of view, since it is considered to be proportional to the intensity $I(t)$ of the luminescence signal produced during the recombination of trapped electrons and positive ions, under certain physical assumptions.

The important experimental implication of the simulations in figures 2(a) and (b) is that the electron survival probability $P(t)$, and the associated luminescence signal $L(t) = -\mathrm{d}P/\mathrm{d}t$ depend on the value of the parameter n_0'. This parameter in turn depends on the initial concentration n_0 of trapped electrons, and on the tunneling length a, according to equation (19). This implies that the loss of charge due to tunneling (and the shape of the luminescence signal associated with it) depend on the prior irradiation dose received by the sample. This important result from the theoretical analysis is further considered in the Discussion section.

Equations (14) and (17) which describe the decay kinetics of trapped electrons in other situations are also simplified in similar ways, by using the reduced initial concentration and the reduced time. Hereafter we use the reduced initial concentration and the reduced time to show graphically the decay kinetics of trapped electrons in various situations.

Figure 3(a) compares the decay kinetics obtained from equation (8*a*) and that obtained from equation (14). In both cases the reduced initial concentration of positive ions is assumed as $m_0' = 0.08$. If the tunneling length is $a = 2 \times 10^{-9}$ m, this value of m_0' corresponds to the initial positive ion concentration $m_0 = 10^{25}$ m^{-3}. The curves shown by full lines are obtained from equation (14) in which the initial concentration of trapped electrons is assumed to be much lower than that of positive ions. On the other hand, the curves shown by the broken lines are obtained from equation (8*a*) in which the initial concentration of trapped electrons is equal to that of positive ions. If one increases the initial concentration of trapped

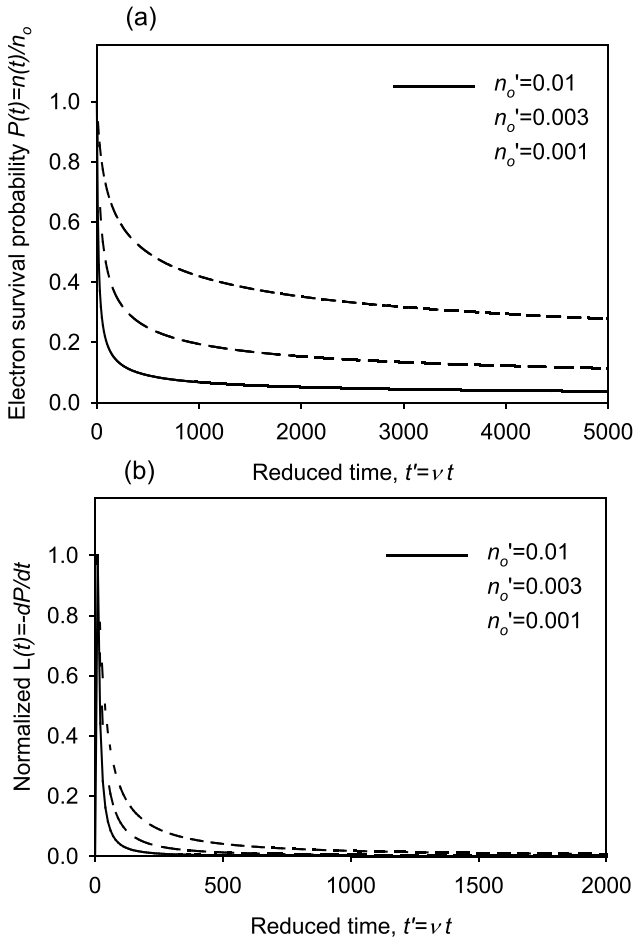

Figure 2. (a) The survival probability $P(t) = n(t)/n_0$ given by equation (19), for three values of the reduced initial concentration of trapped electrons, $n_0' = 0.01$, 0.003 and 0.001. The curves have been normalized at time $t = 1/\nu$. As the value of the parameter n_0' increases, the loss of charge by tunneling becomes faster. Note the use of the reduced time parameter $t' = \nu t$ in the horizontal axis, instead of using the actual time t. (b) The normalized derivative $L(t) = -\mathrm{d}P/\mathrm{d}t$ calculated for the same three values of the reduced initial concentrations of trapped electrons n_0', as in (a).

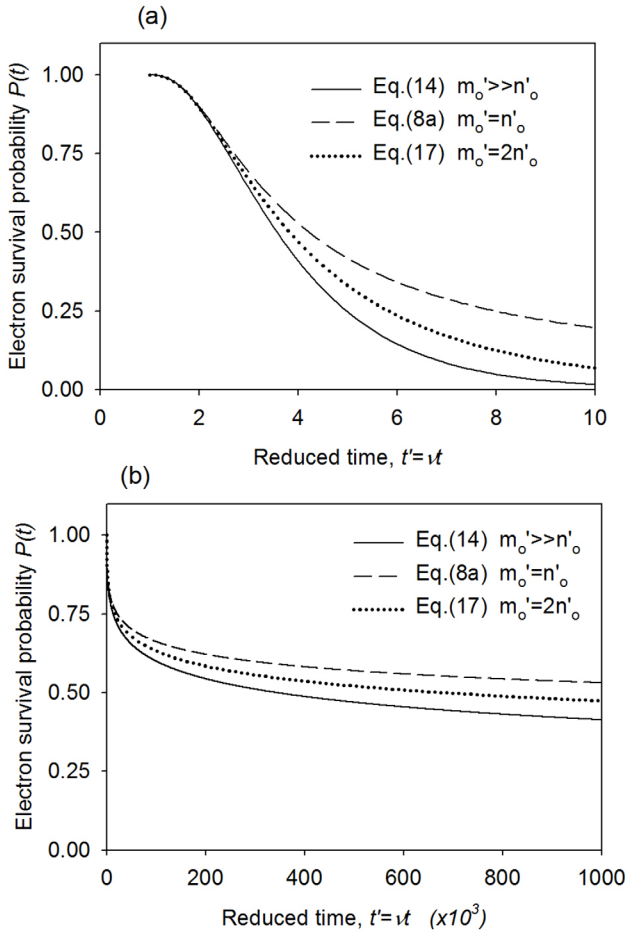

Figure 3. Comparison of tunneling processes occurring under two different physical assumptions. (a) The *dashed* curve represents the analytical equation (8*a*) with reduced initial concentration of positive ions $m_0' = 0.08$, corresponding to a tunneling length $a = 2 \times 10^{-9}$ m and an initial charge density of $m_0 = 10^{25}$ m^{-3}, and under the assumption that the concentrations of electrons and ions are equal at all times. The *solid* curve represents the analytical equation (14), in which the concentration of electrons is assumed much lower than that of ions. The middle dotted curve represents an intermediate case calculated from equation (17), with a ratio of reduced initial concentrations $m_0'/n_0' = 2$. (b) The same simulations as in (a), with a much smaller tunneling length $a = 0.2 \times 10^{-9}$ m.

electrons starting from the case shown by the full line, the decay of positive ions by recombination with trapped electrons become significant. This decreases the concentration of positive ions and as a result slows down the decay of trapped electrons. When the initial concentration of trapped electrons is increased to that of positive ions, the decay curve of trapped electrons approach the broken curve given by equation (8*a*). The middle dotted curve in figure 3(a) represents an intermediate case calculated from equation (17), with a ratio of reduced initial concentrations $m_0'/n_0' = 2$.

Figure 3(b) shows similar decay kinetics obtained for a much smaller value $m_0' = 8 \times 10^{-5}$ of the reduced initial concentration of positive ions. If the tunneling length is $a = 0.2 \times 10^{-9}$ m, this value of m_0' corresponds to an initial defect concentration $m_0 = 10^{25}$ m^{-3}. This much smaller value of a (and n_0') is representative of ground-state tunneling in feldspars and apatites, while the value of a used in figure 3(a) is believed to be more representative of longer range tunneling in these materials, taking place via the excited state of the electron trap [7, 12, 13].

4. Monte Carlo simulations

In this section, the same problem studied analytically in the previous sections is studied by using Monte Carlo simulations.

In a recent paper, Pagonis and Kulp [17] presented a Monte Carlo model in which the concentration of positive ions far exceeds that of electrons. These authors presented Monte Carlo simulations describing the loss of charge due to ground-state tunneling on a wide variety of time scales, from microseconds to thousands of years. Furthermore, they suggested that the model can also be used to describe luminescence signals originating from the nearest-neighbor tunneling mechanism in feldspars, and compared the simulations with experimental data on time-resolved infrared-stimulated luminescence (TR-IRSL) experiments.

In this paper, we use the same Monte Carlo code as described in detail in Pagonis and Kulp [17], and assume again a random distribution of electrons and positive ions in a cube. Figure 4(a)

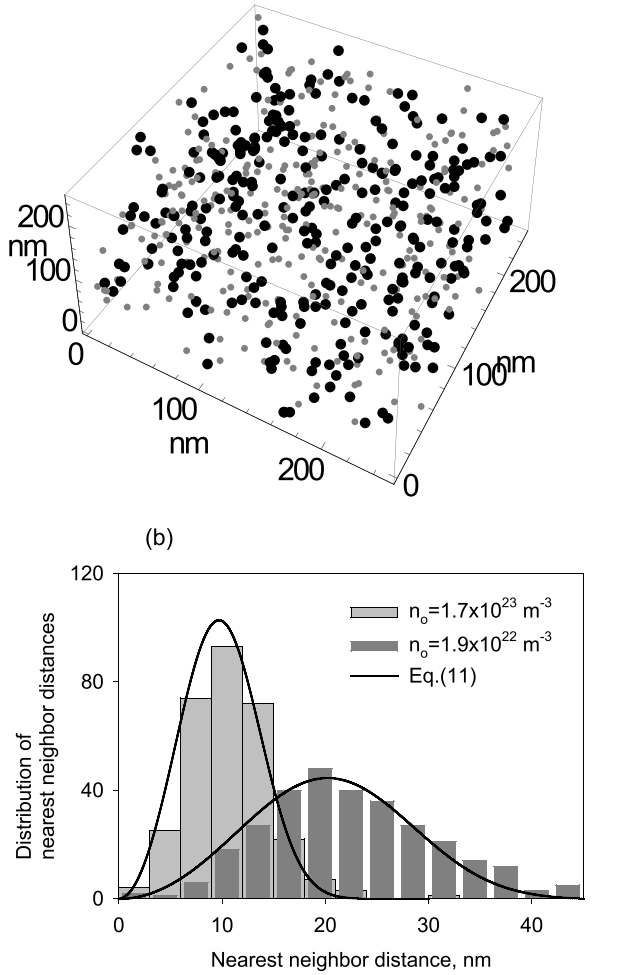

Figure 4. (a) A typical simulated random distribution of 300 electrons (smaller points) and 300 ions (larger points), inside a cube with a side length of $R = 250$ nm. (b) The initial distribution of nearest-neighbor distances in the system at time $t = 0$. The solid line represents the well-known analytical normalized distribution of nearest-neighbor distances inside the cube, equation (20) in the text.

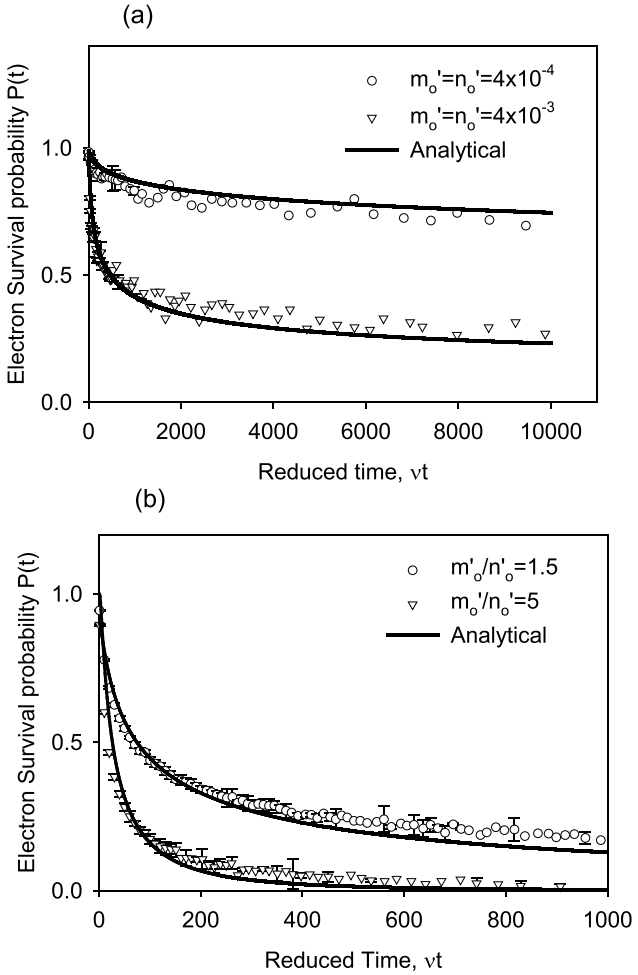

Figure 5. (a) A typical Monte Carlo simulation for a cube with the parameters: $\alpha = 1 \times 10^9$ m^{-1}, $\nu = 10\,\mathrm{s}^{-1}$, and for two values of $n_0' = 4 \times 10^{-13}$, 4×10^{-4}. The circles and triangles represent the average of 100 Monte Carlo simulations, and the error bars represent the standard errors of the mean. Each run consists initially of 300 electrons and 300 positive ions, and the solid lines represent the analytical equation (8*a*). (b) The same type of simulation as in (a), for two different ratios of reduced initial concentrations $m_0'/n_0' = 1.5$ and 5. The solid lines represent the new analytical equation (17).

shows a typical example of such a random distribution of 300 electrons (smaller points) and 300 ions (larger points) inside a cube with a side length of $R = 250$ nm. Figure 4(b) shows the histogram of the initial distribution of nearest-neighbor distances in the system at time $t = 0$ for two different initial concentrations of electrons $n_0 = 1.9 \times 10^{32}$ m^{-3} and $n_0 = 1.7 \times 10^{23}$ m^{-3}. The solid lines in figure 4(b) represent the well-known analytical normalized distribution of nearest neighbors with initial concentration n_0 [1, 17]:

$$g(r) = 4\pi n_0 r^2 \exp[-4\pi n_0 r^3/3]. \qquad (20)$$

By taking the derivative in this equation and setting it equal to zero, the maximum of the distribution of distances is found to occur at $r = 0.542 n_0^{-1/3}$, and the maximum height of this normalized distribution is equal to $1.895 n_0^{1/3}$.

Figure 5(a) shows a typical Monte Carlo tunneling simulation for a cube with the parameters: tunneling length $a = 1 \times 10^{-9}$ m, tunneling frequency $\nu = 1\,\mathrm{s}^{-1}$ and for two values of the reduced initial concentration $n_0' = 4 \times 10^{-3}$, 4×10^{-4}. The individual points (circles and triangles) shown in figure 5(a) represent the average of 100 Monte Carlo simulations, and the errors bars represent the standard errors of the mean for the 100 Monte Carlo runs, with each run consisting initially of 300 electrons and 300 positive ions. The solid line in figure 5(a) represents the analytical equation (8*a*), as described in the previous section. Good agreement is seen between these two approaches, with some rather small differences seen at large times. These observed differences are most likely due to the discrete nature of the Monte Carlo simulations, as opposed to the continuous distributions used in deriving equation (8). Specifically at long times when less than ~20% of electrons are left in the solid, one expects that the Monte Carlo results will be affected by the very small number of particles being simulated. One possible method of improving the agreement between the analytical equation and the Monte Carlo simulations is by increasing the number of simulated number of electrons and positive ions, as well

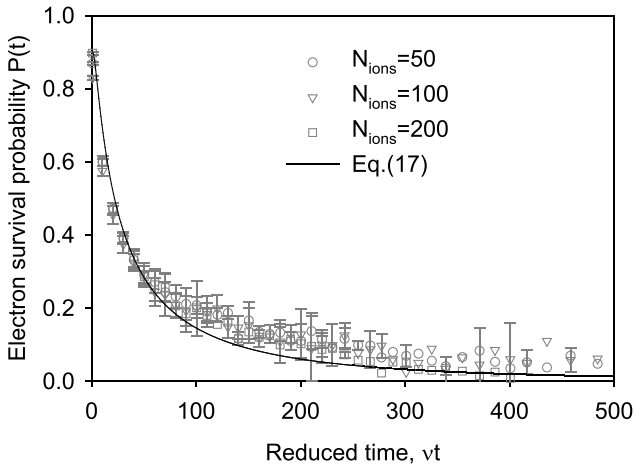

Figure 6. The result of running 100 Monte Carlo simulations with 50, 100 and 200 electrons and ions in the system, while keeping the reduced initial concentration of positive ions constant at $m_0' = 0.001$, and the ratio $m_0'/n_0' = 5$. The results of the Monte Carlo method do not depend on the total number of particles, indicating unbiased statistical results.

as increasing the number of simulated solids. In addition, a more realistic system can be simulated by including periodic boundary conditions in the simulations.

Figure 5(b) shows the same type of results as those of figure 5(a), for two different ratios of reduced initial concentrations $m_0'/n_0' = 1.5$ and 5. The solid lines represent the new analytical equation (17). Again good agreement is seen at each initial concentration.

Figure 6 shows the result of Monte Carlo simulations with $N = 50$, 100 and 200 ions in the cube, while keeping the reduced initial concentration of positive ions constant at $m_0' = 0.001$, and the ratio $m_0'/n_0' = 5$. As the number of particles is varied in these simulations, the size of cube is also varied appropriately, so that the initial concentrations m_0', n_0' stay fixed. Figure 6 shows that the results of the Monte Carlo method do not depend on the total number of particles used in simulations, indicating unbiased statistical results.

5. Discussion and suggestions for experimental work

In this paper we derived two new analytical equations (8*a*) and (17), which describe the electron survival probability $P(t)$ in a random distribution of electrons and ions, with arbitrary relative concentrations of electrons and positive ions in the system. These analytical equations are completely general, and should be valid for any values of the parameters in the model. We now discuss how these new equations could be used for a quantitative analysis of luminescence signals in materials exhibiting tunneling phenomena. Specifically we discuss two experimentally observed types of luminescence signals, *remnant* and *prompt* luminescence signals.

Equations (8*a*) and (17) express the electron survival probability $P(t)$, and can be used to analyze *remnant luminescence signals* in a variety of experiments. For example, it has been well established that feldspars and apatites exhibit the phenomenon of anomalous fading, in which trapped charges are lost progressively over geological times by ground state tunneling. In the laboratory anomalous fading is usually quantified by measuring the *remnant* luminescence signals by using either optically stimulated luminescence experiments (OSL), or by using thermally stimulated luminescence experiments (TL). These remnant TL/OSL signals monitored during anomalous fading experiments represent the signals remaining after various times have elapsed from the end of irradiation. Equations (8*a*) and (17) can be used directly as fitting functions for such remnant luminescence signals, with the reduced concentration n_0' and the tunneling frequency ν representing the two physical parameters extracted from the experimental data.

As discussed above, the quantity $L(t) = -\mathrm{d}P/\mathrm{d}t$ is proportional to the experimentally measured intensity $I(t)$ of the luminescence signal produced during the recombination of trapped electrons and positive ions. Therefore the *derivatives* of equations (8*a*) and (17) can be used to quantity a variety of *prompt luminescence signals* in a variety of experiments. For example, the derivatives of these equations can be used as fitting functions for isothermal luminescence signals measured at a constant temperature (ITL), for infrared stimulated luminescence experiments (IRSL), and perhaps also for long term afterglow luminescence observed in many materials [3].

The second experimental implication of the simulations in this paper is that the electron survival probability $P(t)$, and the associated luminescence signal $L(t) = -\mathrm{d}P/\mathrm{d}t$ depend on the prior irradiation dose received by the sample. For example, there is relevant experimental evidence that the shape of continuous-wave infrared stimulated luminescence (CW-IRSL) signals depends on the prior dose received by the sample, and that it may also depend on the ionization properties of the radiation used [17, 25].

Further experimental work at different irradiation doses is required, in order to ascertain the exact dependence of the remnant and prompt luminescence signals on the irradiation and thermal history of the dosimetric materials exhibiting tunneling.

The new equations derived in this paper could also be useful in analyzing luminescence signals in situations where experimentalists can control the density of defects in the crystal, thus altering the luminescence properties of the material. For example, a variety of dosimetric materials double doped with rare earths of different concentrations have been studied extensively during the past decade [3, 22].

Finally we point out that the Monte Carlo simulations method in this paper can also be extended to the study of nanodosimetric materials, in which the tunneling length a can become of the order of magnitude of the crystal size R. In such materials and for high defect densities, one might expect that the luminescence signals may depend on the size of the nanocrystals, and this effect can be simulated using the Monte Carlo code used in this paper.

References

[1] Tachiya M and Mozumder A 1974 *Chem. Phys. Lett.* **28** 87
[2] Tachiya M and Mozumder A 1975 *Chem. Phys. Lett.* **34** 77
[3] Eeckhout K V, Smet P F and Poelman D 2010 *Materials* **3** 2536–66
[4] Visocekas R, Spooner N A, Zink A and Blank P 1994 *Radiat. Meas.* **23** 371
[5] Li B and Li S H 2008 *J. Phys. D: Appl. Phys.* **41** 225502
[6] Kars R H, Wallinga J and Cohen K M 2008 *Radiat. Meas.* **43** 786
[7] Larsen A, Greilich S, Jain M and Murray A S 2009 *Radiat. Meas.* **44** 467
[8] Poolton N R J, Kars R H, Wallinga J and Bos A J J 2009 *J. Phys.: Condens. Matter* **21** 485505
[9] Pagonis V, Jain M, Thomsen K J and Murray A S 2014 *J. Lumin.* **153** 96–103
[10] Pagonis V, Chen R, Kulp C and Kitis G 2017 *Radiat. Meas.* (https: //doi.org/10.1016/j.radmeas.2017.01.001)
[11] Jain M and Ankjærgaard C 2011 *Radiat. Meas.* **46** 292
[12] Jain M, Guralnik B and Andersen M T 2012 *J. Phys.: Condens. Matter* **24** 385402
[13] Kitis G and Pagonis V 2013 *J. Lumin.* **137** 109–15
[14] Kars R H, Poolton N R J, Jain M, Ankjaergaard C, Dorenbos P and Walling J 2013 *Radiat. Meas.* **59** 103–13
[15] Sfampa I K, Polymeris G S, Pagonis V, Theodosoglou E, Tsirliganis N C and Kitis G 2015 *Nucl. Instrum. Methods Phys. Res.* B **359** 89–98
[16] Polymeris G S, Tsirliganis N, Loukou Z and Kitis G 2006 *Phys. Status Solidi* a **203** 578
[17] Pagonis V and Kulp C 2017 *J. Lumin.* **181** 114–20
[18] Kulkarni R N 1994 *Radiat. Prot. Dosim.* **51** 95–105
[19] Mandowski A and Świątek J 2000 *Synth. Met.* **109** 203–6
[20] Mandowski A 2006 *Radiat. Prot. Dosim.* **119** 85–8
[21] Pagonis V and Kitis G 2012 *Phys. Status Solidi* B **249** 1590–601
[22] Mandowski A and Bos A J J 2011 *Radiat. Meas.* **46** 1376–9
[23] Pagonis V and Chen R 2015 *Radiat. Meas.* **81** 262–9
[24] Pagonis V and Kitis G 2015 *J. Lumin.* **168** 137–44
[25] Morthekai P, Jugina Thomas J, Pandian M S, Balaram V and Singhvi A K 2012 *Radiat. Meas.* **47** 857–63
[26] Sfampa I K, Polymeris G S, Tsirliganis N C, Pagonis V and Kitis G 2014 *Nucl. Instrum. Methods Phys. Res.* B **320** 57–63